esa

ECOSPHERE

Does climate affect pollen morphology? Optimal size and shape of pollen grains under various desiccation intensity

MACIEJ JAN EJSMOND,[1,†] DOROTA WROŃSKA-PILAREK,[2] ANNA EJSMOND,[3] DOMINIKA DRAGOSZ-KLUSKA,[1] MONIKA KARPIŃSKA-KOŁACZEK,[4] PIOTR KOŁACZEK,[5] AND JAN KOZŁOWSKI[1]

[1]*Institute of Environmental Sciences, Jagiellonian University, Gronostajowa 7, 30-387 Kraków, Poland*
[2]*Department of Forestry Natural Foundations, Poznan University of Life Sciences, Wojska Polskiego 71 d, 60-625 Poznan, Poland*
[3]*Faculty of Biology and Earth Sciences, Jagiellonian Univeristy, Gronostajowa 7, 30-387 Kraków, Poland*
[4]*Institute of Botany, Jagiellonian University, Lubicz 46, 31-512 Kraków, Poland*
[5]*Department of Biogeography and Palaeoecology, Faculty of Geographical and Geological Science, Adam Mickiewicz University, Dzięgielowa 27, 61-680 Poznań, Poland*

Citation: Ejsmond, M. J., D. Wrońska-Pilarek, A. Ejsmond, D. Dragosz-Kluska, M. Karpińska-Kołaczek, P. Kołaczek, and J. Kozłowski. 2011. Does climate affect pollen morphology? Optimal size and shape of pollen grains under various desiccation intensity. Ecosphere 2(10):117. doi:10.1890/ES11-00147.1

Abstract. Seed production is likely constrained by pollen limitation and the viability of pollen grains decreases rapidly in time due to water evaporation. Any decrease in the surface-to-volume ratio, through increase in size or change in shape of a grain, reduces the rate of water loss. However, grain size trade-offs with the number of grains that can be produced by a plant. Here, we tested the hypothesis that under higher desiccation stress pollen grains become larger and more spherical. We analyzed data on the pollen morphology of eight *Rosaceae* species and the desiccation intensity based on temperature, potential evapotranspiration and altitude. To explain the mechanisms underlying our results, we present a model that optimizes the size and shape of pollen grains under different conditions. We report that pollen grains under more intense desiccation stress during flowering periods tend to be larger but do not change shape. This conclusion is consistent with the results of a theoretical model presented here. Our report fills a gap in our knowledge about a fundamental process in plant reproduction. We also discuss the significance of our results in light of current palynological and ecological problems (e.g., global climate change).

Key words: desiccation; pollen limitation; pollen production; pollen morphology; pollen shape; pollen size; temperature.

Received 18 May 2011; revised 6 August 2011; accepted 12 August 2011; final version received 7 October 2011; **published** 31 October 2011. Corresponding Editor: D. P. C. Peters.

† **E-mail:** maciek.ejsmond@uj.edu.pl

INTRODUCTION

The production and morphology of pollen grains are key features of pollination biology. In the last decade, pollen limitation, which is influenced by many factors, has emerged as a one of the major forces limiting the fitness of plants and may affect plant life histories (Ashman et al. 2004, Knight et al. 2005). Most research on pollen limitation has concentrated on plant-pollinator interactions (Harder and Aizen 2010), which is an interesting aspect of the pollination story, but if analyzed separately from the context of the abiotic environment has limited power to predict effects of climatic change on pollination processes. Although pollen production of pollen may be strongly constrained by environmental factors (for review see Delph et al. 1997), the

adaptive significance of the inter- and intraspecific variability in the size-number pollen tradeoff and pollen morphology has rarely been analyzed in this context.

The water content of a ripe pollen grain may represent 5–50% of grain mass depending on the species. Higher water content generally corresponds to a higher rate of germination on the stigma and lower tolerance to desiccation during dispersal (Pacini 2000, Pacini et al. 2006). The viability of partially dehydrated pollen, in contrast to pollen with naturally low water content, usually decreases rapidly with water loss (Nepi et al. 2001). It is reasonable to hypothesize that the size and shape of a pollen grain may affect its time to desiccation and, as a consequence, the likelihood of successful pollination under specific environmental conditions.

Palynological books and journals have described significant inter- and intraspecific variability of the size, shape and other morphological characteristics of pollen grains. Even a slight change in grain size has considerable consequences on the number of grains produced if the same amount of resources is used for pollen production.

In this study, we tested whether pollen size and morphology of eight *Rosaceae* species depend on desiccation intensity based on altitude and primary climate variables, such as temperature and potential evapotranspiration (PET) during flowering periods. We hypothesize that under high desiccation stress, pollen grains become larger and more spherical in shape. Increasing in size and becoming more spherical may decrease the surface-to-volume ratio of a grain and therefore reduce the rate of water loss. To explain the mechanisms underlying our results, we present a model that optimizes the size and shape of pollen grains under different conditions. We then discuss our empirical results in light of our theoretical findings.

Materials and Methods

Pollen data

To test our hypothesis, we used pollen grain morphology data for one species of bramble (*Rubus gracilis*, N = the number of individuals from different locations = 13) and five species of roses (*Rosa canina*, $N = 17$; *R. gallica*, $N = 15$; *R. sherardii*, $N = 12$; *R. dumalis*, $N = 9$; *R. rubiginosa*, $N = 8$) (Wrońska-Pilarek and Boratyńska 2005, Wrońska-Pilarek et al. 2006, Wrońska-Pilarek and Jagodziński 2009; Wrońska-Pilarek, *unpublished data*). All pollen samples were acetolysed according to the method described by Wrońska-Pilarek (1998). Pollen trait measurements were based on 50 grains for *R. gallica*, 20 grains for *R. gracillis* and 30 grains for other species. We also included data for two hawthorn species (*Crataegus ambigua*, $N = 6$; *C. monogyna*, $N = 10$), with 30–50 grains being analyzed from each specimen (Oybak Dönmez 2008).

We extracted data on the polar (P) and equatorial (E) axes of pollen grains from published papers or directly measured them (see raw data in Supplement 1). For all studied species, we used these measurements to calculate mean pollen grain surface area (S), volume (V) and the surface-to-volume ratio. We chose to use a spheroid (i.e., ellipsoid with two equal radii, $0.5P$, $0.5E$, $0.5E$) as a geometrical model of a pollen grain with S and V represented by the following:

$$V = \frac{\pi P E^2}{6} \tag{1}$$

$$\text{for } P > E: \quad S = \frac{\pi E^2}{2} + \frac{\pi E P}{2z}\arcsin(z) \text{ where}$$

$$z = \sqrt{1 - \left(\frac{E}{P}\right)^2} \tag{2a}$$

$$\text{for } P < E: \quad S = \frac{\pi E^2}{2} + \frac{\pi P^2}{2z}\log\left(\frac{1+z}{1-z}\right) \text{ where}$$

$$z = \sqrt{1 - \left(\frac{P}{E}\right)^2} \tag{2b}$$

$$\text{for } P = E: \quad S = \pi(P)^2 \tag{2c}$$

(*public communication*; http://mathworld.wolfram.com/Spheroid.html).

Climate data and flowering date

To correlate pollen morphology with climatic conditions, we used data on the flowering periods of the specimens and the altitude, monthly mean temperature and PET of the collection sites (see raw data in Supplement 1).

All *Rosa* and *Rubus* species specimens were

collected in Poland (Appendix). We used coordinates provided by D. Wrońska-Pilarek and topographical maps of Poland and official Polish Government websites (e.g., http://www.geoportal.gov.pl/) to locate *Rosa* and *R. gracilis* specimens. We were unable to find coordinates of sites for a substantial number of *Crataegus* specimens, and so we used only the altitude data provided by E. Oybak Dönmez for this analysis.

We applied elevation data from the Shuttle Radar Topography Mission 90-m Digital Elevation Model (Jarvis et al. 2008) with the resolution of the grid ca. 250×250 m (latitude $\times$ longitude). The mean monthly temperature (Hijmans et al. 2005) and monthly PET data between the years 1950 and 2000 (Trabucco and Zomer 2009) had a resolution of ca. 0.55×1 km. All geographic data were processed in ArcGis 9.3 (Environmental Systems Research Institute, Redlands, California, USA).

The flowering periods for *R. gracilis* were determined based on when flowering specimens were collected. Because the available temperature and PET data were monthly means and because some specimens were collected at different times throughout a particular month, we calculated the weighted mean temperature of a 31-day period so that the day of collection was in the middle of this period. For example, if a plant was collected on May 5, the temperature was calculated as $(5 + 15)$/31 May temperature + 11/31 April temperature. Because we did not know the precise collection dates for a substantial number of *Rosa* specimens, the flowering periods were obtained from the literature: May and June for *R. canina* and *R. dumalis*; June and July for *R. gallica* and *R. sherardii*; and May, June and July for *R. rubiginosa* (Popek 2002).

Statistical analysis

To obtain the independent variables that best describe pollen size and sensitivity to desiccation, we performed Principal Component Analysis (PCA) for five continuous pollen grain variables: P, E, $\log_{10}(V)$, $\log_{10}(S)$, surface-to-volume ratio and P/E ratio. Pollen volume and surface area were log-transformed to assure linearity between variables (Quinn and Keough 2002). We also performed a PCA for three climate variables to obtain a variable that best described the joint trends in evaporation rate, temperature and altitude. To test the relationship between the principal components of pollen grain characteristics and components extracted from climatic variables we used General Linear Model with species as a fixed factor.

The model

To address how temperature affects the size, shape and number of viable pollen grains delivered to stigmas, we modeled the optimal allocation of resources to the production of pollen grains. In our model, a pollen grain is a spheroid characterized by the P and E axes and the volume (V) and surface area (S) of the grain calculated according to Eqs. 1–2c. In the numerical examples, presented in the *Model results* section, the volume of a grain cannot be smaller than one cubic unit. The size of pollen grains is optimized by maximizing the fitness measure F: the expected number of pollen grains reaching the ovule, taking into account the competitive abilities at two pollination stages (pollen germination and pollen tube growth rate). The assumed fitness measure consists of three components. The first component is the expected number of grains (N) produced by a plant and is represented by the following equation:

$$N(P,E) = \frac{\mathrm{En}}{V(P,E)} \tag{3}$$

where En is a constant pool of energy available for reproduction. In the numerical examples (see *Results*: *Model results*) the amount of energy available for reproduction was set to 10^{10}. The En value does not affect the optimization results because we are interested in relative fitness and not the precise number of grains that successfully fertilize ovules. Eq. 3 reflects a primary trade-off (i.e., grain size vs. grain number).

The second fitness component describes the life expectancy of a grain as a function of size, shape and temperature transformed to the chances of reaching the stigma. We assume for simplicity that the viability of a grain depends only on water content, which decreases due to evaporation.

We modeled the rate of water loss by adopting a parameterized model of maize pollen dehydration (Aylor 2003, Aylor et al. 2005). The driving force for water loss in the model is the

vapor pressure difference between the evaporation surface of a pollen grain and the ambient air outside the grain. The instantaneous rate of water loss from a grain can be expressed as:

$$\frac{dW}{dt} = -kS(C_c - C_a) \quad (4)$$

where W is the mass of water in the pollen grain while C_c and C_a describe the concentrations of water vapor on the evaporation surface of the pollen grain and in the surrounding air, respectively. The conductance for water loss of the pollen wall and surrounding boundary layer of air k was set to an arbitrary small value, equal to 10^{-5} in the results presented below (see *Results*: *Model results*). Such a low value of k indicates that our arbitrary time unit is very small. By applying the thermodynamic relationship between concentration and vapor pressure and expressing the water content relative to dry weight, $\theta = W/m_d$, we obtain

$$\frac{d\theta}{dt} = \frac{-kSM_w p_0(T)}{m_d R(T + 273.15)} \left(h_r(\theta) - \mathrm{RH}/100\right) \quad (5)$$

(for detailed transformation see formulas 2–4 in Aylor 2003). Eq. 5 describes the rate of water loss from a grain with dry weight m_d in temperature T (°C) and at relative air humidity RH (%) where M_w and R are constants (molecular weight of water and gas constant, respectively), p_0 is the saturation vapor pressure at temperature T, and h_r is the 'effective' relative humidity inside the wall of the pollen grain. The relative humidity h_r can be expressed by the following equation:

$$h_r = \exp\left(\frac{-a\theta^{-b}D_w}{R(T + 273.15)}\right) \quad (6)$$

where D_w is the molar volume of water. Coefficients describing water potential at the evaporating surface, a and b, were taken from Aylor 2003 and are equal to 3.218 and 1.35, respectively (see methods in Aylor 2003 for details of the calculation of these coefficients).

Eq. 5 indicates that pollen loses water only as long as $h_r > \mathrm{RH}/100$. The empirical data indicate that at 23.5°C, the equilibrium water content θ for maize pollen at RH = 20, 33, 54 and 75% was equal to 4.4, 5.8, 8.9 and 15.7%, respectively (Aylor 2003). In order to parameterize the dehydration process in our model we assumed that the dry weight of the grain is proportional to its volume, $m_d = nV$, where n is the scaling constant. We then adjusted the value of n so as to obtain values of θ close to the equilibrium water content (after a long finite time interval) for maize pollen at temperature and relative humidity reported by Aylor (2003).

In our model, the time scale is arbitrary and the rate of water loss over time depends only on the conductance coefficient k and the water content of pollen. The initial relative water content, defined as W/m_d, was set to $\theta_0 = 0.5$ which is approximately equivalent to 30% of the total mass of ripe pollen. Although pollen grains tolerate loss of water during transport, if their water content is low then the phospholipid structure of their cell membranes changes from a lamellar or liquid crystalline form to a gel state and is extremelly vulnerable to irreversible changes in membrane structure which are directly responsible for pollen grain death (Taylor and Hepler 1997). Thus pollen grain viability dramatically decreases when the water content declines to low values (see Fig. 3 in Aylor 2003). We assume, for simplicity, a critical relative water content $\theta_{Crit} = 0.06$ for the results presented in the *Model results* section. Under this low value for water content, the chances of germination for a maize pollen grain are negligible (ca. 0.005% relative to the germination chances of a fully hydrated grain) (Aylor 2003, Aylor et al. 2005). We assumed such a conservative value of θ_{Crit} so as to assure the robustness of the results of the model and to account for species-specific differences in tolerance to dehydration stress (Nepi et al. 2010). The accepted threshold at which the cell dies in our model is relatively low and corresponds to a considerable decrease in pollen grain viability even in species highly tolerant to pollen dehydration stress, e.g., *Petunia hybrida* (Nepi et al. 2010).

Our model infers a scenario in which the actual air humidity is low enough to drive pollen grain cells to desiccation and death. The empirical data suggest that a considerable decrease in pollen viability may be expected for humidity levels even up to 50% (Aylor 2003, Aylor et al. 2005, Nepi et al. 2010). Across this range of RH the selection pressure forced by water loss is still strong. RH therefore does not affect the qualitative results of our model for species tolerant to pollen dehydration stress. Thus to keep our

report concise we did not model the effect of the variability in actual air humidity on pollen life expectancy, and for results presented below we assume RH = 30%.

To determine the expected time of grain viability, we compute L, the time period necessary to decrease the water content from θ_0 to $\theta_{Crit,}$ by solving numerically Eq. 5 with Ordinary Differential Equations solver ode113 implemented in MATLAB 7.9 (Mathworks, Natick, Massachusetts, USA).

We assume that pollen delivery to stigmas is due to pollinator visits. To account for this, we transform grain life expectancy (L) into the cumulative probability that a grain of a certain size will reach a stigma during the time period L when it is still viable. For example, in a hypothetical scenario, a pollinator visits a flower of a pollen donor plant and then visits other flowers. If we discretize time to short intervals, which represent a precise approximation because of a very fine time scale, there is some chance (p) that a grain is delivered to a stigma and also some chance (q) that the grain will not fall from the insect to the stigma and be lost during this time interval. Therefore, the probability that a grain will reach a stigma in a certain time period is given by a geometric series with the common ratio $q(1-p)$ and the first term pq. Therefore, the cumulative probability of successful pollen delivery (Z) during period L depends nonlinearly on time and can be calculated according to following formula:

$$Z(P,E,T) = pq\frac{(q(1-p))^{L+1}-1}{q(1-p)-1}. \qquad (7)$$

Empirical data show that the cumulative chance of landing on a conspecific stigma is usually smaller than 1% for a particular pollen grain (Harder and Johnson 2008). Because the time scale in our model is arbitrary, we use pairs of q and p that satisfy the condition $\underset{L\to\infty}{Z} = 0.01$. Changing p in these pairs affects the rate of increase of the cumulative chance of a pollen grain landing on a stigma within the given time, as illustrated in Fig. 1. Under high p, the chance limit of 1% is quickly approached and is approached more slowly with a small p. Because an increase in temperature results in a shortening of L, the cumulative probability of reaching a stigma before a grain's death is higher for a large

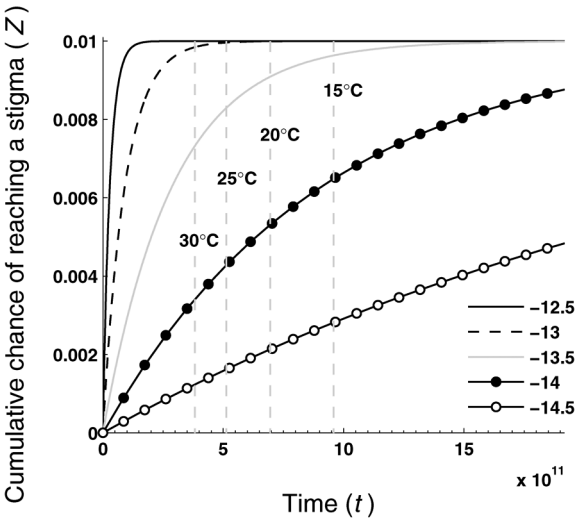

Fig. 1. Effect of changes in the chance of pollen loss during transport on the dynamics of the pollination process. The chance of successful pollination, p, per 1 time unit (log-transformed values given in legend) reflects the value of q, the chance of pollen grain loss during transport (see *Materials and Methods*: *The Model*). Vertical gray dashed lines indicate the life expectancy of a spherical grain with $P = E = 25$ units for the temperature given at a line, while the x-axis limit was set equal to the life expectancy of a grain with $P = E = 50$ units at 15°C.

than for a small p (Fig. 1). By manipulating q, we investigated the effect of the dynamics of pollen transport on the shape and size of pollen grains. Such dynamics have recently been shown to be a crucial factor in shaping the variability in pollen dispersal (Richards et al. 2009).

The third fitness component, U, describes the chances of winning the competition to reach an ovule and is inversely related to the time necessary for a pollen grain to germinate (t_G) and to reach the ovary by the pollen tube (t_V).

$$U = \frac{1}{t_G + t_V}. \qquad (8)$$

For germination, the grain is hydrated through its surface after falling on the stigma. We assume that the rate of hydration (W) is proportional to the part of the grain surface sticking to the stigma $S_G(P, E)$:

$$\frac{dW}{dt} = S_G(P,E) \qquad (9)$$

where t is time in arbitrary units and S_G denotes the area of sticking surface. After solving Eq. 9, we obtain t_G, the time period necessary to increase in water content from the initial level, a_1V, to the level a_2V, which triggers pollen germination:

$$t_G = \frac{a_2V(P,E) - a_1V(P,E)}{S_G(P,E)}. \quad (10)$$

The initial and final water levels do not affect the qualitative results of the model and were set to $a_1 = 0.3$ (equivalent to θ_0 in Eqs. 5 and 6) and $a_2 = 1$ for the results presented in the *Model results* section. We assume a conservative estimate of the expected water content at germination equal to the initial water content, a_1, because changing the water content at germination does not influence the results of our model. To account for the fact that a spheroid with $P/E \neq 1$ sticks to the stigma with a larger surface area than a sphere of the same volume, we compute S_G assuming that the surface sticking to the stigma is limited by the plane intersecting the spheroid perpendicularly to E (for a prolate spheroid) or P (for an oblate spheroid) and crossing 95% of the radius of P or E, respectively (Fig. 2). Because of the complicated form of the analytic formula for the area, we calculate S_G using numerical methods implemented in MATLAB by J. Rosenberg (*public communication*; http://www-users.math.umd.edu/~jmr/241/surfint.html).

In our model, the rate of pollen tube growth depends on grain volume, which is generally empirically justified (Cruden 2009). The length of the pollen tube (M) changes according to the following formula:

$$\frac{dM}{dt} = a_4V^{\alpha}. \quad (11)$$

Bigger grains usually have higher pollen tube growth rates, while a_4 is a scaling constant and the exponent $\alpha \in \langle 0, 1 \rangle$ allows us to model the allometric character of the relationship between pollen volume and tube growth rate. After solving Eq. 11, we obtain t_V, the time necessary to reach the ovule by the pollen tube:

$$t_V = \frac{h}{a_4V^{\alpha}} \quad (12)$$

where h is the distance between the stigma surface and ovary. According to Eq. 8, U, the third fitness component measuring the chance for successful pollination, is inversely proportional to the cumulative time of germination and pollen tube growth. In our model, h was set to 1 and a_4 to 10^{-7}. The values of the scaling constants h and a_4 do not affect the qualitative results because all units in the model are arbitrary. During the natural pollination process, the time of germination of a grain is usually much shorter than the time of pollen tube growth, so t_G is always smaller than t_V. Setting a_4 to 10^{-7} results in realistic values of the t_G/t_V ratio for optimal pollen.

The fitness measure in our model, Eq. 13, is a product of three components: (1) the number of grains that can be produced from a constant amount of resources, Eq. 3, (2) grain life expectancy transformed to the chances of reaching a conspecific stigma, Eq. 7, and (3) the chances of winning the competition during germination and pollen tube growth, Eq. 8:

$$F(P,E,T) = N(P,E)Z(P,E,T)U(P,E). \quad (13)$$

Because of the complexity of the fitness formula, we used numerical algorithms to find the values of P and E that maximize fitness at a given temperature for prolate and oblate pollen grains (see Fig. 3A for example). We then compared the results calculated for different temperatures (see Fig. 3B for example). All calculations were performed with MATLAB 7.9. The code for the model is provided in the Supplement 2.

Results

Empirical results

The PCA for pollen grain characteristics displayed a pattern that was consistent for all studied groups. Two components extracted by the PCA explained over 99% of variance in all cases and had an eigenvalue >1. The pollen principal components for all analyzed species can be easily interpreted in general terms of pollen grain morphology (Table 1). Higher pollen PC1 ($PC1_{poll}$) values suggest bigger pollen grains and smaller surface-to-volume ratios with almost no change in shape. As the pollen PC2 ($PC2_{poll}$) value increases, there is a substantial change in grain shape as defined by an increase in the P/E ratio. The change in shape is achieved mostly by an increase of the P axis with a slight change in

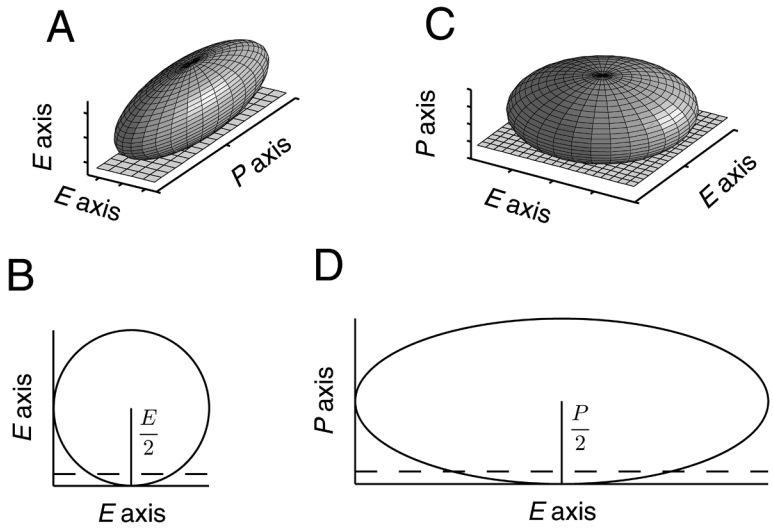

Fig. 2. Scheme for the calculation of the part of the ellipsoid sticking to the stigma, S_G. Panels A–B and C–D show schemes for prolate and oblate pollen grains landing on a stigma surface (gray plane). Panels B and D show the intersection of ellipsoids by the plane (dashed line). The sticking surface, S_G, is the part of surface of the ellipsoids below the plane. The plane divides the polar (for oblate grains) or equatorial radius (for prolate grains) in such a way that 5% of the radius length is below the plane.

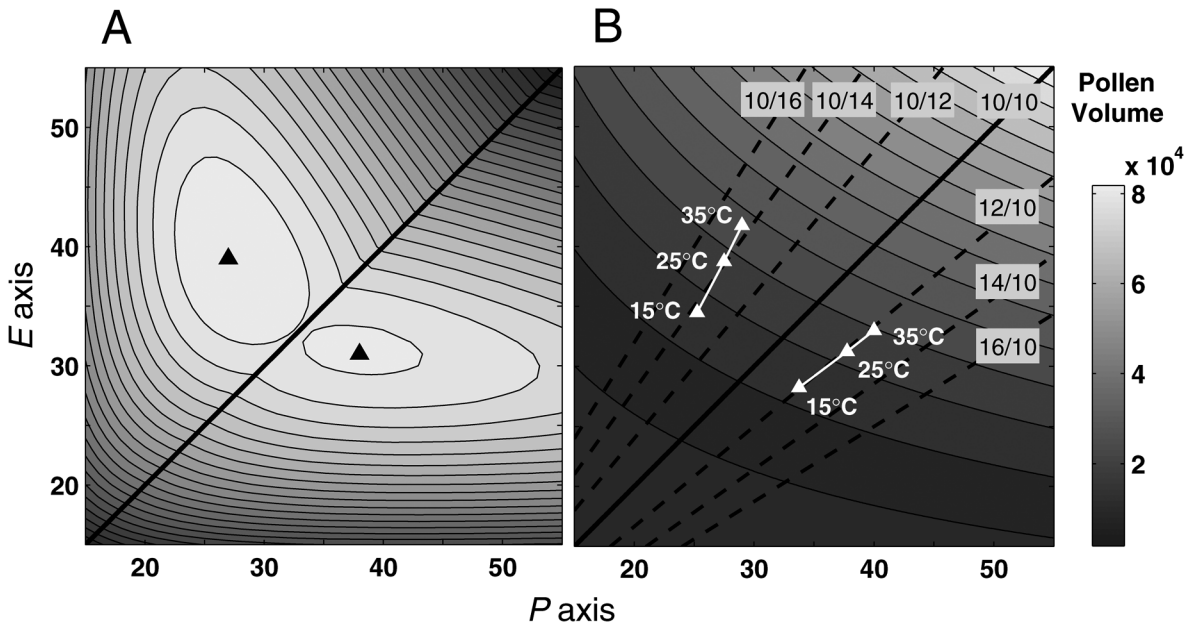

Fig. 3. (A) An exemplary fitness landscape: black triangles mark the location of optimal pollen grain dimensions at a temperature of 25°C. (B) The effect of temperature on optimal pollen grain volume and shape. The black solid line indicates the separation of prolate (below the line) and oblate (above the line) pollen grains. Dashed isolines mark 6 exemplary *P*/*E* ratios. White lines connecting triangles show the location change of optimal volume and shape in temperatures from 15 to 35°C. Model parameters: $p = 10^{-14}$ and $\alpha = 0.95$.

Table 1. Loadings of pollen grain traits on pollen principal components (PCs).

Trait	*Rosa*		*Rubus*		*Crategus*	
	PC1	PC2	PC1	PC2	PC1	PC2
P	0.893	0.450	0.896	0.442	0.959	0.280
E	0.974	−0.217	0.973	−0.228	0.996	−0.067
P/E	−0.153	0.988	−0.154	0.988	−0.252	0.967
$\text{Log}_{10}(V)$	1.000	−0.003	1.000	0.000	1.000	0.019
$\text{Log}_{10}(S)$	1.000	0.024	1.000	0.026	1.000	0.007
S/V	−0.997	0.060	−0.999	0.047	−0.996	−0.016
Eigenvalue	4.76	1.23	4.77	1.23	4.96	1.02
VE (%)	79.39	20.49	79.50	20.45	82.75	16.99

Note: VE is the percentage of variance explained by PC.

the surface-to-volume ratio and no change in pollen volume. For the climatic variables of altitude, PET and temperature in the flowering period, the PCA extracts one PC with an eigenvalue >1. Climate PC1 ($PC1_{clim}$) can be easily interpreted in terms of desiccation stress (Table 2): a high $PC1_{clim}$ indicates high desiccation pressure. The species analyzed here have different pollen grain shapes; *Rosa* and *Rubus* have prolate grains ($P/E > 1$; a high $PC2_{poll}$ corresponds to a less spherical shape) while *Crataegus* grains are oblate ($P/E < 1$; low $PC2_{poll}$ corresponds to a more spherical shape).

Rubus gracilis.—Pollen size, in contrast to shape, is positively related to desiccation pressure ($PC1_{poll}(PC1_{clim})$: $F_{1,11} = 5.37$, $P = 0.041$; $PC2_{poll}(PC1_{clim})$: $F_{1,11} = 1.01$, $P = 0.336$).

Rosa.—We detected a positive relationship between pollen size and desiccation pressure ($PC1_{poll}(PC1_{clim})$: $F_{1,51} = 9.70$, $P = 0.003$). The analyzed *Rosa* species differed with respect to $PC1_{poll}$ ($F_{4,51} = 2.69$, $P = 0.041$), and *R. gallica* has significantly larger pollen grains than the other species ($P < 0.001$, Duncan test). There is also a slight but non-significant difference in the responses of $PC1_{poll}$ to $PC1_{clim}$ between species (species × $PC1_{clim}$: $F_{4,51} = 2.34$, $P = 0.068$). Pollen shape is not correlated with climate ($PC2_{poll}(PC1_{clim})$: $F_{4,51} = 2.16$, $P = 0.148$) and does not differ between species ($F_{4,51} = 0.89$, $P = 0.477$).

Table 2. Loadings of climate variables on climate principal component 1 (PC1).

Climate variable	*Rosa* PC1	*Rubus* PC1
Altitude	−0.761	−0.877
Temperature	0.969	0.978
PET in flowering period	0.942	0.897
Eigenvalue	2.40	2.53
VE (%)	80.11	84.32

Note: VE is the percentage of variance explained by PC.

Crategus.—*Crategus ambigua* has bigger pollen grains than *C. monogyna*, and therefore $PC1_{poll}$ differs between species ($F_{1,12} = 6.62$; $P = 0.024$). Pollen grain size decreases with altitude ($PC1_{poll}$(altitude): $F_{1,12} = 5.11$; $P = 0.043$). There is no significant interaction between altitude and species with respect to $PC1_{poll}$ ($F_{1,12} = 2.11$; $P = 0.172$), and grain shape ($PC2_{poll}$) is not related to altitude ($F_{1,12} = 0.61$; $P = 0.451$). Species do not differ in $PC2_{poll}$ ($F_{1,12} = 0.46$; $P = 0.513$).

In summary, empirical results show that pollen grains are larger when under intense desiccation stress for the three analyzed groups. There was no change pollen grain shape with desiccation stress.

Model results

Under different dynamics of pollen transport (p) and efficiencies of the conversion of grain volume into the pollen tube growth rate (α), the maximal fitness on the polar-equatorial axis plane indicates pollen grains with an optimal size and shape (Fig. 3A). The position of the fitness maxima for both prolate and oblate grains depends on temperature and the combination of α and p. As shown in Fig. 3B, temperature mostly affects the size of the optimal pollen grain and only slightly affects the shape (white lines in Fig. 3B) for an exemplary combination of α and p; however, the shape is not spherical. The same is true for a broad range of parameters as discussed below. To understand how the fundamental grain characteristics change within the parameter space, we transformed the locations of the fitness

maxima on the polar-equatorial axis plane into pollen volume and P/E ratio, which indicate the grain size and shape, respectively.

Optimal pollen volume and shape under different transport dynamics (p) and the benefits of grain size for pollen tube growth (α).—The volume of a pollen grain with both axes being optimal increases monotonically with a decrease in p (Fig. 4A). If the chances for landing on a conspecific stigma increase slowly with time, as for low p (Fig. 1), it is better to produce larger pollen grains that can stay alive long enough before critical desiccation to reach the stigma. Therefore, for a high p, the optimal pollen size is relatively small (Fig. 4A), and it will have a high likelihood for successful pollination (Fig. 4B).

The effect of α on optimal grain volume depends on the level of p (Fig. 4A). For the majority of assumed values of p, the optimal pollen volume is achieved at an intermediate value of α. As indicated by dashed lines in Fig. 4A the maximal pollen volume for a given p moves toward lower values of α with a decrease in p. This is because under low p, the increase in pollination chance over time is slow (Fig. 1) and the change in the pollination chance with a decrease in size is relatively small (compare Figs.4A and 4B). The number of grains produced is inversely related to grain volume, and under higher efficiencies of the conversion of grain volume into the growth rate of the pollen tube (high α), the better tactic is to produce smaller and more numerous grains than grains with a large volume. Despite the smaller volume, optimal grains at high α have a shorter time of pollen tube growth (t_V) because of higher conversion efficiencies of grain volume into pollen tube growth rate (filled surface on Fig. 4C).

Because the volume of a grain affects its life expectancy, and optimal volume depends on α as well as other factors, the second fitness component (Z) indirectly depends on α, although α is not an argument of Z. Similarly, the third fitness component (U) indirectly depends on p in two ways: first, the rate of increase in pollination chance with time influences the volume of an optimal grain and, because of this, also changes the time of pollen tube growth (t_V); and second, grains with a long life expectancy must be large and may be constrained by the germination time (t_G) because of their size.

The shape of an optimal grain depends on both α and p. For a very steep increase in pollination chance (high values of p) and low efficiency of transformation of pollen volume to tube growth rate (low values of α), optimal grains are spherical. For low values of p and high values of α, grains tend to be more prolate or oblate in shape. This does not seem intuitive because a prolate or oblate shape increases the desiccation rate, and we expect that such shapes should be selected against under conditions in which pollination chance increases slowly over time. However, with a slow increase in pollination chance, an efficient tactic in terms of avoiding desiccation is to produce large grains. Enlarged pollen may be constrained by germination time (Fig. 4C), and this is why small optimal pollen grains tend to be more spherical in shape than large grains in our model (compare Fig. 4A and D). Therefore, desiccation is a minor factor affecting the optimal pollen shape because a grain with a high volume compared to one with a small volume is more restricted by the surface-to-volume ratio during germination. For a steep increase in pollination chance with time, the best tactic is to produce numerous grains that have a relatively short time of germination and are spherical and therefore less vulnerable to desiccation.

The effect of temperature.—As depicted in Fig. 4A, it is always a better strategy to produce larger grains as temperature increases. Because a larger size does not fully compensate for increased desiccation rates at higher temperatures, grains have less of a chance for successful pollination at higher temperature for all values of p and α (Fig. 4A). The relative change in volume, shape and the length of the short and long axes as a response to temperature is presented in Fig. 5. Temperature has the strongest effect on the size and dimensions of optimal grains. In the middle range of values of p over a broad range of α values, the optimal pollen volume at 30°C is almost twice that of the volume of an optimal grain at 15°C, and the linear dimensions for both prolate and oblate pollen are ca. 30% higher. In contrast to the change in the volume and length of the axes of an optimal pollen grain as an adaptive response to increased temperature, the shape changes only slightly and for a limited

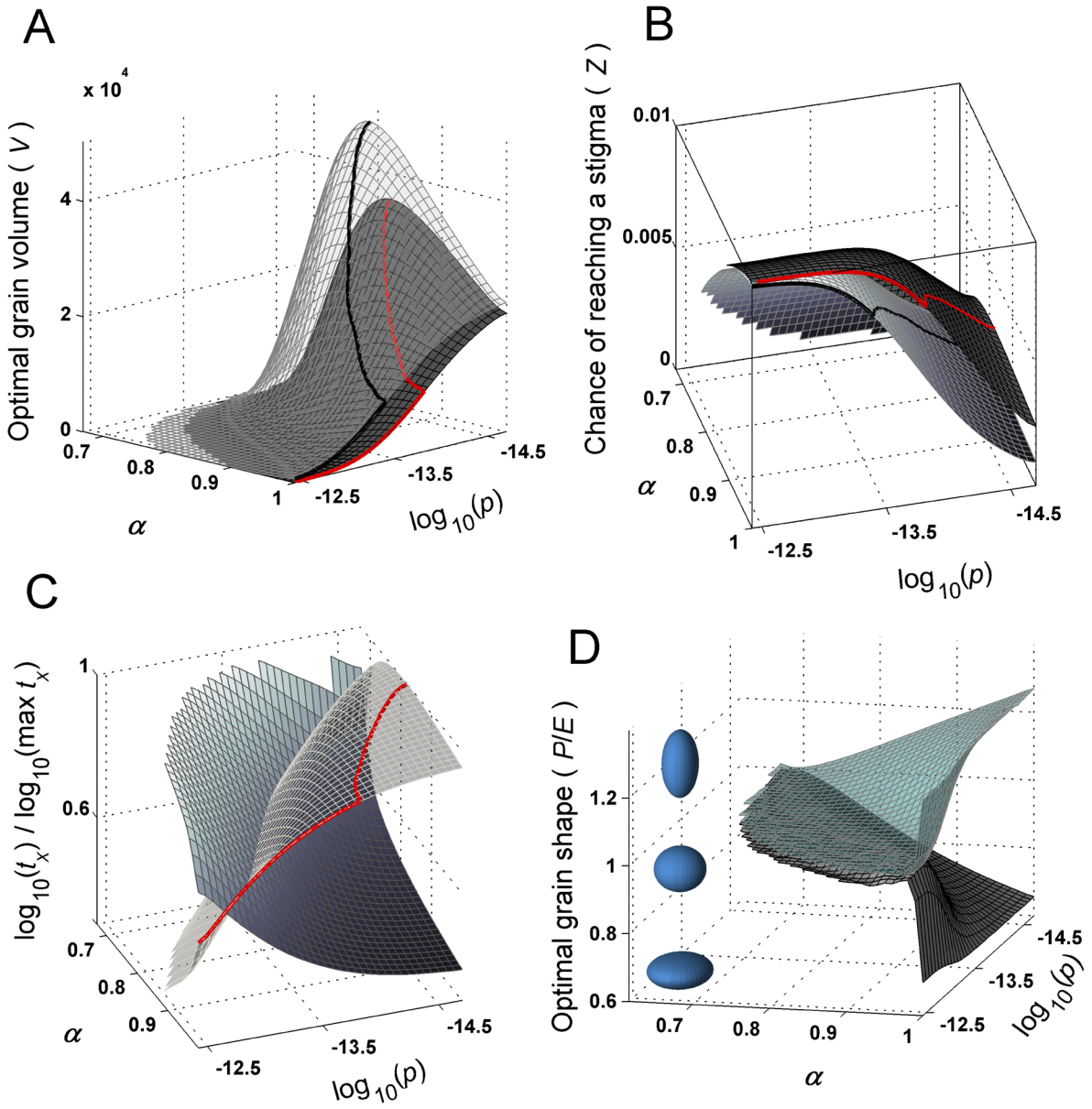

Fig. 4. The optimal volume, two fitness components, and shape of a pollen grain as a function of p and α. (A) The optimal volume of a prolate pollen grain at two temperatures: 15°C (filled) and 30°C (transparent surface). Note that grains are always larger at higher temperatures. (B) The chance of successful pollination for a prolate pollen grain at 15°C (dark gray) and 30°C (light gray shaded surface). Note that the surface for higher temperatures is always below the surface for lower temperatures over the entire parameter space. (C) Third fitness component U of a prolate pollen grain at 15°C decomposed to time of germination, t_G (transparent surface), and growth time of the pollen tube, t_V (filled surface). For better visibility, both t_G and t_V were $\log_{10}$-transformed and normalized to their maximal values. (A–C) Thick solid lines link maximal V, Z and t_G of an optimal grain calculated for a given temperature and p value across different α. The optimal volume and two fitness components Z and U of oblate pollen grains show a very similar pattern. (D) The optimal shape of a pollen grain at 15°C as a function of p and α. The transparent surface corresponds to grains with prolate shape, while the filled surface corresponds to oblate grains.

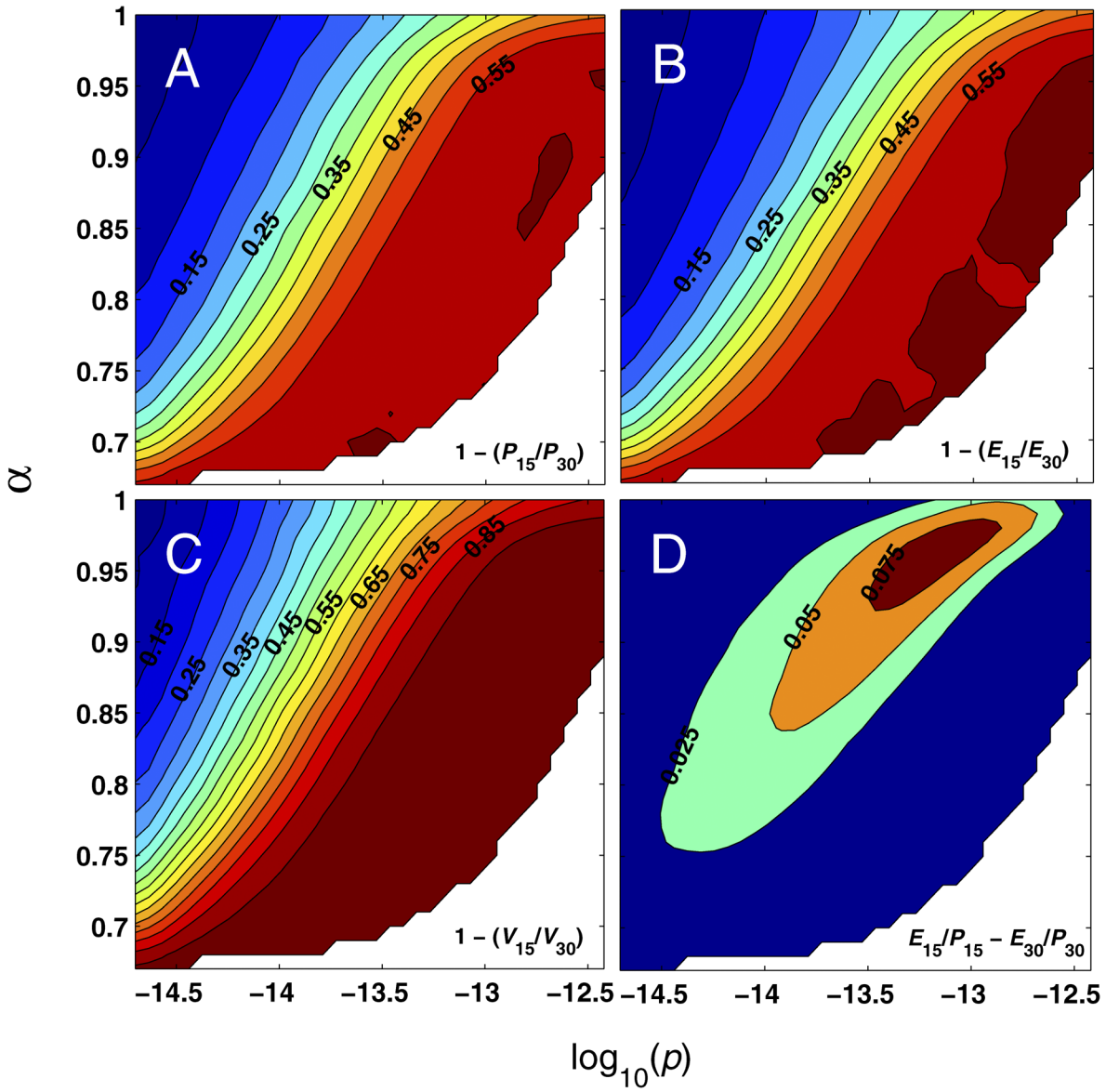

Fig. 5. The change in dimensions, volume and shape of an optimal prolate pollen grain in response to temperature. Isolines show the relative change for 4 pollen grain characteristics: polar axis (A), equatorial axis (B), volume (C) and shape expressed as the ratio of the shorter to the longer axis (D). The pattern was similar for oblate pollen grains. Surfaces where slightly smoothed with discrete cosine transform method (Garcia 2010) to reduce numerical round-off errors.

range of parameters. As temperature increases, the optimal size increases and the shape tends to be less spherical for both prolate and oblate grains. It may not seem intuitive that the shape is less spherical as desiccation pressure increases because a sphere has the lowest surface-to-volume ratio; however, under higher temperatures, grains are larger, which decreases the surface-to-volume ratio, and the change in shape toward being less spherical, to some extent, offsets the increase of germination time characteristic for large grains (see Eq. 10).

Discussion

Here, we present the first evidence that a fundamental life history trait for plants, i.e., pollen production, is closely connected to environmental temperature through the optimization of the number and size of grains produced. In contrast, temperature does not significantly affect pollen shape. Our theoretical model reveals a possible mechanism behind this relationship, and it also explains why pollen grains are usually prolate or oblate and not spherical and why temperature affects pollen volume more than pollen shape. The connection of temperature with pollen size and the number of pollen grains links aspects of pollen production with an easily measured environmental variable and fills a gap in our knowledge about a fundamental process in plant reproduction. The described relationship is relatively simple in contrast to other aspects of pollination biology that result from plant-pollinator co-evolution. The simple character of this relationship may facilitate studies on the mechanisms responsible for the shifts in plant species geographical ranges due to global climate change observed in the last decade (Lenoir et al. 2008).

Consequences of the model's assumptions

To keep the model simple we assume that the change in the probability of reaching a stigma is not dependent on the temperature (see Fig. 1). However, classic empirical studies show that the visitations to a flower by ectothermic pollinators are, to some extent, temperature dependent (Arroyo et al. 1985). Thus the effect on pollen size requires further studies.

In our model, a grain sticks to a stigma with a surface of S_G during germination. We calculate the sticking surface to account for the slight deformation of the pollen grain and stigma surface after pollen falls onto the stigma and the synthesis of the pollen coat by the stigma (Edlund et al. 2004). When calculated in this manner, the sticking surface (S_G) is not simply proportional to the pollen surface (S). Under a simple mode of proportionality of the sticking surface to the whole surface of an ellipsoid, only a spherical shape would be optimal. Therefore, in our model, the optimality of grains that differ in shape from that of a sphere is related to the assumption that spheroidal grains germinate faster than spherical grains of the same volume. The method to calculate S_G used here does not influence the conclusion regarding the optimal increases in pollen size with temperature.

Phenotypic plasticity or genetic polymorphism?

The most basic question arising from our work, which has primary importance in the context of the response of plant species to global climate change, is whether the observed adaptive reaction of pollen size to desiccation pressure is an effect of polymorphism in genes encoding pollen grain traits or phenotypic plasticity. Despite the limitations of our empirical data, we found a significant intraspecific relationship of pollen size with desiccation pressure. Therefore, we believe that phenotypic plasticity likely underlies the observed relationship; nevertheless, further studies are necessary to answer this question, and common garden experiments may be helpful for this. It will also be worthwhile to check if an increase in pollen grain volume corresponds with an increase in desiccation pressure at an interspecific level.

Explaining the heteromorphism of pollen grain shape

In heteromorphic species, a single plant produces pollen grains that differ in type. For example, species of *Viola* differ in aperture number within a single plant. Such heteromorphism, as described by Dajoz et al. (1991), results in a trade-off between pollen grain pore number and life expectancy: an increase in aperture number is linked to faster germination and a lower life expectancy. Temperature-driven pollinator activity positively correlates with the mean aperture number (Dajoz 1999), and the heteromorphism was suggested to be an evolutionarily stable strategy when two or more species deliver pollen to flowers (Till-Bottraud et al. 1994, Till-Bottraud et al. 2001).

Many plant species produce pollen grains that are variable in shape, ranging from slightly oblate to slightly prolate. Such variability can also be observed in grains produced by a single plant, e.g., *Sorbus aucuparia*, *Rubus rosaefolius* and *Fragaria vesca* (P. Kołaczek, *personal observation* based on reference slides in the collection of the Władysław Szafer Institute of Botany, Polish Academy of Science). For some combinations of

the model's parameters, the optimal shape was close to sphere (Fig. 4D) for both prolate and oblate grains, suggesting that the fitness maxima for those two pollen types are relatively close to each other on the polar-equatorial axis plane. We can easily imagine additional factors, such as differences in the efficiency of transport by different insect species, that could lead to the evolutionary stability of such heteromorphism of pollen grain shapes.

Using pollen size to reconstruct past climate conditions

This report provides a rationale to develop palynological methods that can be used to determine spatial and temporal changes of environmental temperature and aridity with relatively high resolution. By measuring the distribution of pollen grains of a given species deposited in geological layers, we will be able to infer changes in environmental conditions. Although the concept is simple, there are several issues that must be addressed before such a method can be implemented. Here, we discuss only a few examples of these problems to stimulate discussion on this subject. First, because of methodological limitations, deposited grains can be identified only at a relatively high taxonomic level, so changes observed in the size of deposited grains may be caused by changes in the relative frequency of species rather than adaptive changes in the morphology of pollen produced by a single species. Thus, studies must first be conducted to show that the described relationships are true at an interspecific level. Second, sedimentary processes likely disturb the original grain size distributions, so using such information should be preceded by detailed evaluation of the influence of sedimentation on the size of deposited pollen. Third, sedimentary processes may reflect temporal variation in the pollen spectra caused by stochastic effects of pollen deposition and can also be easily changed by the long-distance transport of pollen from different sites.

Conclusions

Based on our theoretical findings, we show that avoiding desiccation by producing pollen grains of an optimal size and shape affects the number of grains produced. This leads to complex results, which can be simply described as a general trend of plants in environments with higher temperatures and PET to produce less numerous and larger pollen grains and to exhibit a slight change in grain shape, which may be more difficult to detect. Further studies are necessary to determine if knowing the size of pollen grains can significantly improve our predictions on the impact of climate change on plant populations and to reconstruct past environmental conditions.

Acknowledgments

This work was partly supported by the Polish Ministry of Science and Higher Education (grant N N304 044237) and Jagiellonian University funds (grant DS/WBiNoZ/INoŚ/757/08). We thank Marcin Czarnołęski, Krzysztof Piątek and Paweł Koteja for comments on earlier versions of the manuscript and E. Oybak Dönmez for providing altitude data for the analyzed hawthorn species. A. Ejsmond and M.J. Ejsmond thank all people involved in taking care of their 1-year old son during preparation of the manuscript.

Literature Cited

Arroyo, M. T. K., J. J. Armesto, and R. B. Primack. 1985. Community studies in pollination ecology in the high temperate Andes of central Chile II. The effect of temperature on visitation rates and pollination possibilities. Plant Systematics and Evolution 149:187–203.

Ashman, T. et al. 2004. Pollen limitation of plant reproduction: ecological and evolutionary causes and consequences. Ecology 85:2408–2421.

Aylor, D. E. 2003. Rate of dehydration of corn (*Zea mays* L.) pollen in the air. Journal of Experimental Botany 54:2307–2312.

Aylor, D. E., B. M. Baltazar, and J. G. Schoper. 2005. Some physical properties of teosinte (*Zea mays* subsp. *parviglumis*) pollen. Journal of Experimental Botany 56:2401–2407.

Cruden, R. W. 2009. Pollen grain size, stigma depth, and style length: the relationship revisited. Plant Systematics and Evolution 278:223–238.

Dajoz, I., I. Till-Bottraud, and P. Gouyon. 1991. Evolution of pollen morphology. Science 253:66–68.

Dajoz, I. 1999. The distribution of pollen heteromorphism in *Viola*: ecological and morphological correlates. Evolutionary Ecology Research 1:97–109.

Delph, L. F., M. H. Johannsson, and A. G. Stephenson. 1997. How environmental factors affect pollen performance: ecological and evolutionary perspec-

tives. Ecology 78:1632–1639.
Edlund, A. F., R. Swanson, and D. Preuss. 2004. Pollen and stigma structure and function: the role of diversity in pollination. The Plant Cell. 16:S84–S92.
Garcia, D. 2010. Robust smoothing of gridded data in one and higher dimensions with missing values. Computational Statistics and Data Analysis 54:1167–1178.
Harder, L. D., and M. A. Aizen. 2010. Floral adaptation and diversification under pollen limitation. Philosophical Transactions of the Royal Society B 365:529–543.
Harder, L. D., and S. D. Johnson. 2008. Function and evolution of aggregated pollen in angiosperms. International Journal of Plant Sciences 169:59–78.
Hijmans, R. J., J. L. Cameron, J. L. Parra, P. G. Jones, and A. Jarvis. 2005. Very high resolution interpolated climate surfaces for global land areas. International Journal of Climatology 25:1965–1978.
Jarvis, A., H. I. Reuter, A. Nelson, and E. Guevara. 2008. Hole-filled seamless SRTM data V4, International Centre for Tropical Agriculture (CIAT). http://srtm.csi.cgiar.org/
Knight, T. M., J. A. Steets, J. C. Vamosi, S. J. Mazer, M. Burd, D. R. Campbell, M. R. Dudash, M. O. Johnston, R. J. Mitchell, and T. Ashman. 2005. Pollen limitation of plant reproduction: pattern and process. Annual Review in Ecology, Evolution and Systematics 36:467–497.
Lenoir, J., J. C. Gégout, P. A. Marquet, P. DeRuffray, and H. Brisse. 2008. A significant upward shift in plant species optimum elevation during the 20th century. Science 320:1768–1771.
Nepi, M., G. C. Franchi, and E. Pacini. 2001. Pollen hydration status at dispersal: cytophysiological features and strategies. Protoplsma 216:171–180.
Nepi, M., L. Cresti, M. Guarnieri, and E. Pacini. 2010. Effect of relative humidity on water content, viability and carbohydrate profile of *Petunia hybrida* and *Cucurbita pepo* pollen. Plant Systematic and Evolution 284:57–64.
Oybak Dönmez, E. 2008. Pollen morphology in Turkish *Crataegus* (*Rosaceae*). Botanica Helvetica 118:59–70.
Pacini, E. 2000. From anther and pollen ripening to pollen presentation. Plant Systematics and Evolution 222:19–43.
Pacini, E., M. Guarnieri, and M. Nepi. 2006. Pollen carbohydrates and water content during development, presentation, and dispersal: a short review. Protoplasma 228:73–77.
Popek, R. 2002. Róże dziko rosnące Polski: klucz–atlas. Plantpress, Kraków, Poland. [In Polish.]
Quinn, G. P., and M. J. Keough. 2002. Experimental design and data analysis for biologists. Cambridge University Press, Cambridge, UK.
Richards, S. A., N. M. Williams, and L. D. Harder. 2009. Variation in pollination: causes and consequences for plant reproduction. The American Naturalist 174:382–398.
Taylor, L. P., and P. K. Hepler. 1997. Pollen germination and tube growth. Annual Review of Plant Physiology and Plant Molecular Biology 48:461–491.
Trabucco, A., and R. J. Zomer. 2009. Global aridity index (Global-Aridity) and global potential evapotranspiration (Global-PET) geospatial database. CGIAR Consortium for Spatial Information. http://www.cgiar-csi.org/
Till-Bottraud, I., D. L. Venable, I. Dajoz, and P. Gouyon. 1994. Selection on pollen morphology: a game theory model. The American Naturalist 144:395–411.
Till-Bottraud, I., P. Gouyon, D. L. Venable, and B. Godelle. 2001. The number of competitors providing pollen on a stigma strongly influences intraspecific variation in number of pollen apertures. Evolutionary Ecology Research 3:231–253.
Wrońska-Pilarek, D. 1998. Pollen morphology of the polish species of the genus *Ribes* L. Acta Societatis Botanicorum Poloniae 67:275–285.
Wrońska-Pilarek, D., and K. Boratyńska. 2005. Pollen morphology of *Rosa gallica* L. (*Rosaceae*) from southern Poland. Acta Societatis Botanicorum Poloniae 74:297–304.
Wrońska-Pilarek, D., T. Maliński, and J. Lira. 2006. Pollen morphology of Polish species of genus Rubus—Part I. *Rubus gracilis*. Dendrobiology 56:69–77.
Wrońska-Pilarek, D., and A. M. Jagodziński. 2009. Pollen morphological variability of Polish native species of *Rosa* L. (*Rosaceae*). Dendrobiology 62:71–82.

APPENDIX

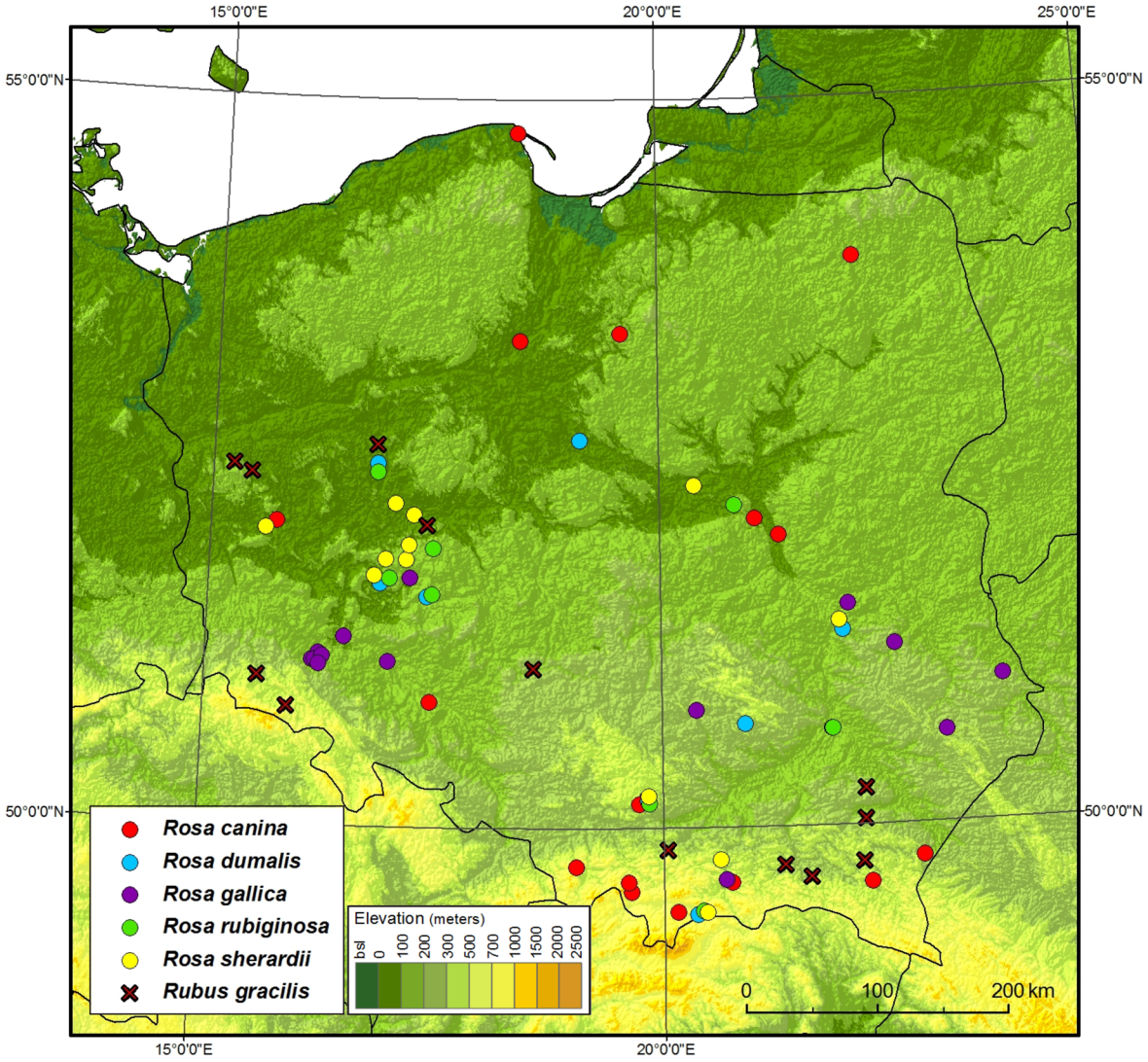

Fig. A1. Collection localities of *Rubus gracilis* and *Rosa* specimens used in the analysis.

SUPPLEMENT 1

The raw data on pollen morphology and climate variables of the collection sites used in the analysis (*Ecological Archives* C002-010-S1).

SUPPLEMENT 2

The MATLAB source code containing the optimization algorithm of pollen morphology used in this paper, and a short description of the program (*Ecological Archives* C002-010-S2).